Review of Scientific Instruments

RESEARCH ARTICLE | MARCH 22 2024

Femtosecond fluorescence conical optical parametric amplification spectroscopy

Ennan Cui ; Heyuan Liu ; Zhuan Wang; Hailong Chen ; Yu-Xiang Weng

Rev. Sci. Instrum. 95, 033008 (2024)
https://doi.org/10.1063/5.0197254

AIP Publishing

Review of Scientific Instruments ARTICLE pubs.aip.org/aip/rsi

Femtosecond fluorescence conical optical parametric amplification spectroscopy

Cite as: Rev. Sci. Instrum. 95, 033008 (2024); doi: 10.1063/5.0197254
Submitted: 12 January 2024 • Accepted: 29 February 2024 •
Published Online: 22 March 2024

Ennan Cui,[1,2] Heyuan Liu,[1,2] Zhuan Wang,[1] Hailong Chen,[1,2,3,a)] and Yu-Xiang Weng[1,2,3]

AFFILIATIONS

[1] The Laboratory of Soft Matter Physics, Beijing National Laboratory for Condensed Matter Physics, Institute of Physics, Chinese Academy of Sciences, Beijing 100190, China
[2] School of Physical Science, University of the Chinese Academy of Sciences, Beijing 100049, China
[3] Songshan Lake Materials Laboratory, Dongguan, Guangdong 523808, China

[a)] **Author to whom correspondence should be addressed:** hlchen@iphy.ac.cn

ABSTRACT

Parametric superfluorescence (PSF), which originated from the optical amplification of vacuum quantum noise, is the primary noise source of femtosecond fluorescence non-collinear optical parametric amplification spectroscopy (FNOPAS). It severely affects the detection limit of FNOPAS to collect the femtosecond time-resolved spectra of extremely weak fluorescence. Here, we report the development of femtosecond fluorescence conical optical parametric amplification spectroscopy (FCOPAS), aimed at effectively suppressing the noise fluctuation from the PSF background. In contrast to traditional FNOPAS configurations utilizing lateral fluorescence collection and dot-like parametric amplification, FCOPAS employs an innovative conical fluorescence collection and ring-like amplification setup. This design enables effective cancellation of noise fluctuation across the entire PSF ring, resulting in an approximate order of magnitude reduction in PSF noise compared to prior FNOPAS outcomes. This advancement enables the resolution of transient fluorescence spectra of 4-dicyanomethylene-2-methyl-6-p-dimethylaminostyryl-4H-pyran (DCM) dye molecules in ethanol, even at an optically dilute concentration of 10^{-6} mol/l, with significantly enhanced signal-to-noise ratios. This improvement will be significant for extremely weak fluorescence detection on the femtosecond time scale.

I. INTRODUCTION

Ultrafast time-resolved fluorescence spectroscopy has been extensively used as a direct and powerful tool for studying ultrafast photophysical and photochemical processes in condensed phases.[1–13] With nonlinear optical laser sampling techniques such as fluorescence up-conversion,[14–18] optical Kerr gating,[19–22] transient grating,[23] and fluorescence non-collinear optical parametric amplification spectroscopy (FNOPAS),[24–29] a time resolution comparable to the excitation laser pulse width can be obtained, which is beneficial for monitoring the fluorescence dynamics occurring on the femtosecond to picosecond time scales. Fluorescence measurement with such high temporal resolution also allows the direct observation of ultrafast coherent exciton dynamics in molecular aggregates and, therefore, is proposed to be an attractive complement of two-dimensional spectroscopy to study quantum coherence effects.[30,31]

Compared with other nonlinear optical techniques, FNOPAS has the unique advantages of both ultra-broad spectral bandwidth (>200 nm) and extremely high optical gain (~10^6).[32] As a consequence, it can record ultrafast broadband fluorescence spectra with a detection limit lower than 20 photons/pulse for noncoherent seeding fluorescence.[32,33] This technique has been successfully used to study diverse ultrafast phenomena, such as delayed fluorescence in semiconductor nanostructures,[34] ultrafast energy transfer in photosynthetic and artificial photosynthetic systems,[35,36] and lasing dynamics in organic waveguides.[27] Despite these advantages, the FNOPAS measurement still suffers from an unavoidable interference from the concomitant parametric superfluorescence (PSF) background,[37] which is generated through a spontaneous parametric down-conversion (SPDC) process between vacuum quantum fluctuation and a pump beam in a nonlinear crystal.[38–40] The PSF background always coincides with the amplified fluorescence signal, both temporally and spatially, and can hardly be removed physically. Consequently, the intensity fluctuation of PSF always introduces considerable noise to the amplified fluorescence signal, which limits this technique to detect extremely weak fluorescence. Mao *et al.* reported the development of a femtosecond FNOPAS

assisted with a 32-channel lock-in amplifier for efficient rejection of the PSF background, allowing the time-resolved fluorescence measurement of rhodamine 6G dye in an ethanol solution at an optically dilute concentration of 10^{-5} mol/l.[37]

In this study, we present a novel technique termed femtosecond fluorescence conical optical parametric amplification spectroscopy (FCOPAS), designed to enhance the suppression of noise fluctuations arising from the PSF background. Departing from the conventional lateral fluorescence collection and dot-like parametric amplification method employed in FNOPAS, FCOPAS utilizes an inventive conical fluorescence collection and ring-like amplification scheme. To elucidate the spatial fluctuation properties of the PSF ring, we conduct measurements involving the correlation of intensity fluctuations between two arbitrarily chosen segments from the PSF background. Our findings affirm the stochastic nature of the PSF ring, allowing for the cancellation of noise fluctuations to some extent through the ring-like amplification scheme. Consequently, the PSF noise is substantially suppressed when compared to the FNOPAS method. This technological advancement enables the resolution of transient fluorescence spectra for 4-dicyanomethylene-2-methyl-6-p-dimethylaminostyryl-4H-pyran (DCM) dye molecules in ethanol, even at an optically dilute concentration of 10^{-6} mol/l, with a markedly improved signal-to-noise ratio. The reduction in PSF noise enhances the precision of femtosecond time-resolved fluorescence measurements, providing a clearer and more detailed understanding of ultrafast phenomena in photochemical and photophysical processes.

II. EXPERIMENTAL SETUP

The schematic diagram of the typical FCOPAS setup is shown in Fig. 1(a). The femtosecond laser (~100 fs pulse duration, 810 nm central wavelength, and 2 kHz repetition rate) is generated by a Ti: sapphire laser system (Spitfire Ace, Spectra Physics). The output beam is first frequency-doubled in a 2 mm thick β-barium borate (BBO) crystal for second harmonic generation (SHG). The generated 400 nm pulses are then split by a beam splitter (BS) with a splitting ratio of 1:4 (T:R). The reflected beam is used as the pump beam for the optical parametric amplification (OPA), and the transmitted beam is used as the excitation beam to excite the sample. The pump beam (~100 μJ/pulse) is focused by a plano-convex lens (f = 300 mm) on a 2 mm thick BBO crystal used for the OPA, and the excitation beam (~0.7 μJ/pulse) is focused on the sample to emit fluorescence. Then, the generated fluorescence is collected and focused on the BBO crystal to overlap with the pump beam for the OPA process. A long-pass filter is employed to remove the residual 400 nm excitation light.

Traditionally, a lateral fluorescence collection and dot-like parametric amplification scheme is generally employed in FNOPAS [Fig. 1(b)].[32,33] In this scheme, the collected fluorescence from the sample is injected into the BBO crystal with a specific propagation direction, and the non-collinear angle α between the pump beam and the fluorescence beam is generally around 3.9°.[33] As a consequence, the amplified fluorescence signal appears as a bright point located on the PSF ring, as shown in Fig. 1(b).

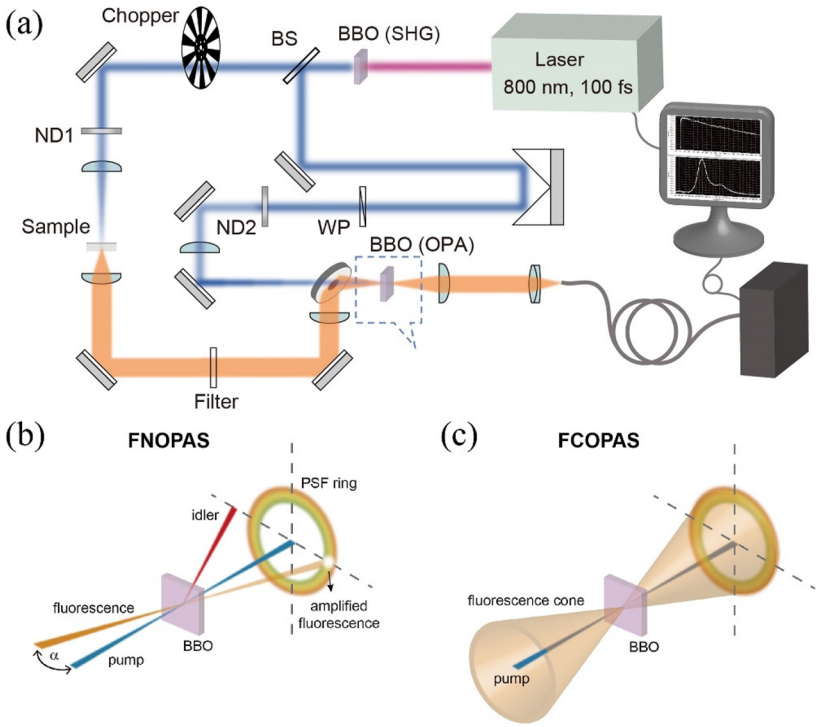

FIG. 1. (a) The schematic diagram for the FCOPAS setup. BS: 1:4 (T:R) beam splitter, WP: λ/2 wave plate at 400 nm, ND1 and ND2: neutral density filters, BBO (SHG) is cut at $\theta = 29.2°$, and BBO (OPA) is cut at $\theta = 31.7°$. (b) The schematic diagram for the lateral collection and dot-like amplification scheme in traditional FNOPAS. (c) The schematic diagram for the cone-shaped collection and ring-like amplification scheme used in FCOPAS.

Based on the principle of the OPA process, all the light injected into the BBO crystal with the propagation direction satisfying the phase-matching condition can be amplified. That means we can simultaneously amplify all the collected fluorescence, which propagates with a fixed non-collinear angle α to the pump beam. Therefore, we here introduce a conical fluorescence collection and ring-like amplification scheme [Fig. 1(c)] to replace the one used in traditional FNOPAS [Fig. 1(b)]. To achieve this, a mirror with a through-hole in the center is employed to converge the collected fluorescence along with the propagation direction of the pump beam, and both beams are concurrently focused on the BBO crystal [Fig. 1(a)]. As a consequence, a conical zone of the fluorescence beam at the phase matching angle can be parametrically amplified, and the rest is blocked. With this optical configuration, all the fluorescence located on the PSF ring can be amplified simultaneously. As a result, not only the fluorescence collection and amplification efficiencies but also the signal-to-noise ratio can be greatly improved, which will be discussed later.

After passing through the OPA crystal, the pump beam is blocked, and all the amplified fluorescence is collected. The PSF background (I_{PSF}) originating from the SPDC process always coincides with the amplified fluorescence signal (I_{flu}) because both of them obey the same phase-matching condition.[37] To remove the PSF background, we modulate the excitation beam to 1 kHz through an optical chopper. Then, the spectra of the amplified signal with ($I_{PSF} + I_{flu}$) and without (I_{PSF}) the seeding fluorescence are recorded by a fiber-coupled spectrometer (AvaSpec-ULS2048CL-EVO, Avantes). As a result, the spectra of the pure amplified fluorescence signal I_{flu} can be obtained.

The time delay between the pump and the excitation beams was controlled by a monitored delay stage. The half-wave plate WP is used to realize the phase-matching condition of FCOPAS by rotating the polarizations of the pump beam. The neutral density filters ND1 and ND2 are placed to adjust the excitation and the pump intensities, respectively. The DCM ethanol solution was used as the fluorescent sample. During the measurement, the DCM solution was continuously stirred in the sample cell with an optical path length of 1 mm. All measurements were performed at room temperature.

III. RESULTS AND DISCUSSION

A. Suppression of the PSF intensity fluctuation

Since the PSF background originates from the optical amplification of the vacuum quantum noise, the intensity fluctuations within the PSF ring are supposed to exhibit spatial uncorrelation. As displayed in Fig. 2(a), fluctuations observed at distinct points (A, B, or C) along the PSF ring are expected to be random. Therefore, when aggregating signals across the entire PSF ring [Fig. 1(c)], the noise fluctuations from different points on the ring tend to partly cancel out, resulting in a notable reduction in PSF noise compared to the FNOPAS method [Fig. 1(b)].

To validate the stochastic nature of the PSF ring's spatial properties, we measured the correlation of intensity fluctuations between two small arc segments arbitrarily taken from the ring. Initially, Fig. 2(b) illustrates the statistical properties of the PSF probed at 600 nm derived from segment A in Fig. 2(a), gathered over a 1-s

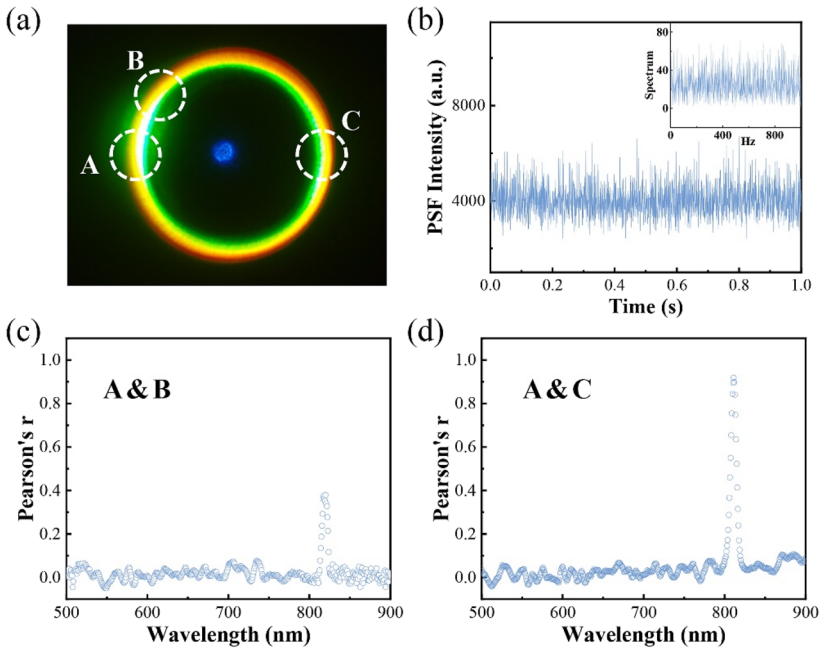

FIG. 2. (a) Far-field image of the PSF Ring, with three distinct arc segments labeled as A, B, and C, respectively. (b) The intensity fluctuation of PSF segment A at 600 nm, recorded over a 1-s trajectory (2000 data points). Inset: the amplitude spectrum of the intensity fluctuation demonstrates nearly flat characteristics resembling white noise across the entire frequency spectrum. (c) and (d) Wavelength-dependent correlations in PSF intensity fluctuations between segment pairs A&B (c) and A&C (d).

trajectory (2000 data points). Its amplitude spectrum displays near-flat characteristics akin to white noise across the entire frequency spectrum. Subsequently, we examined the correlation in intensity fluctuations between segment pairs A&B and A&C.

Mathematically, there are several definitions for the correlation coefficient, which quantifies the relationship between two random variables.[41] Here, we introduce the Pearson product-moment correlation coefficient (Pearson's r) to portray the correlation of co-frequency light intensity fluctuations between different segment pairs. Pearson's r is mathematically defined as

$$\frac{Cov(X,Y)}{\sqrt{D(X)D(Y)}} = \frac{E(XY) - E(X)E(Y)}{\sqrt{D(X)D(Y)}}, \quad (1)$$

where the expectations, variances, and covariance of the random variables X and Y are represented by $E(X)$, $E(Y)$, $D(X)$, $D(Y)$, and $Cov(X, Y)$, respectively.

Figures 2(c) and 2(d) illustrate the wavelength-dependent correlations in PSF intensity fluctuations between segment pairs A&B and A&C, respectively. Notably, only at wavelengths near 800 nm, where the signal and idler lights degenerate with the same photon energy, does Pearson's r for two arbitrary arc segments significantly exceed zero. In particular, when comparing two segments that precisely correspond to a pair of signal and idler lights, such as A&C, their intensity fluctuations exhibit a perfect linear relationship [Fig. 2(d)]. These results confirm that within the PSF, intensity fluctuations are entirely spatially uncorrelated across the entire nondegenerate spectral region, as indicated by Pearson's r values approaching zero. Consequently, for the cone-shaped collection and ring-like amplification scheme utilized in FCOPAS, averaging across the entire ring yields a significant reduction in PSF intensity fluctuation.

Directly and fairly comparing the PSF intensity fluctuations between the lateral collection and dot-like amplification scheme in traditional FNOPAS and the cone-shaped collection and ring-like amplification in FCOPAS is technically challenging. Such a comparison necessitates extensive modifications to the optical setup during measurements, and the results would heavily rely on the optimization of the corresponding optical configurations. To mitigate this deviation, we maintained a fixed optical configuration similar to that used in FCOPAS [Fig. 1(a)]. By exclusively collecting a small segment of the PSF ring and blocking the rest, this approach effectively simulates the traditional FNOPAS method, which solely amplifies a dot region on the PSF ring.

Figure 3(a) presents a comparative analysis of spectra between the PSF segment and PSF ring, revealing significantly higher intensity in the collected PSF ring. Here, the fluorescence is intentionally blocked before reaching the BBO (OPA), allowing the pump beam to exclusively generate the PSF signal. To collect the arc-shaped segment of the PSF, an aperture diaphragm selectively confines a segment approximately one-fifth the size of the entire ring [see Fig. 3(a)]. Meanwhile, Fig. 3(b) illustrates a comparison of noise levels between these two schemes. Here, the noise level is quantified as the standard deviation of the intensity fluctuation divided by the average intensity. Notably, amplification across the entire PSF ring substantially diminishes the PSF noise when contrasted with amplification limited to a portion of the ring. Across most spectral regions, the noise level decreases from above 0.1 to below 0.05. This outcome aligns with expectations, given that the entire circular PSF area is roughly five times larger than the collected arc region. This estimation implies that after spatial averaging, the noise level will decrease by approximately the square root of 5 (~2.2), consistent with the results in Fig. 3(b).

Importantly, in practical FNOPAS measurements, only a point-like area on the PSF ring is typically amplified,[37] which is significantly smaller than the arc-shaped region depicted in Figs. 3(a) and 3(b). As a consequence, it becomes evident that the FCOPAS method offers substantial noise level suppression compared to FNOPAS, leading to significantly enhanced signal-to-noise ratios in practical fluorescence amplification measurements. In particular, achieving a noise level of less than 0.05 through the FCOPAS method could result in a substantial reduction of the PSF background to less than 1/1000 with 5-s averaging (2500 pairs of pulses), representing an approximate order of magnitude increase compared to the previous FNOPAS result.[37]

B. Transient fluorescence spectra of DCM ethanol solution

To validate the feasibility of the FCOPAS method, we initially conducted measurements on the transient fluorescence spectra of

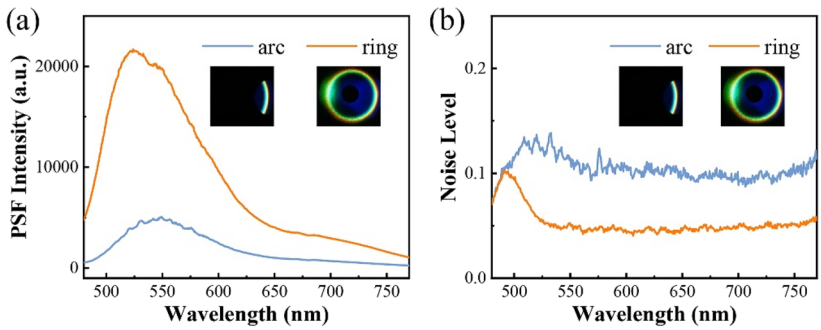

FIG. 3. (a) PSF spectra for the arc-shaped segment (blue line) and the entire ring (orange line), along with the corresponding far-field images. (b) The comparison of noise levels for the arc-shaped segment (blue line) and the entire ring (orange line). It indicates that the amplification across the entire PSF ring can substantially reduce the PSF noise.

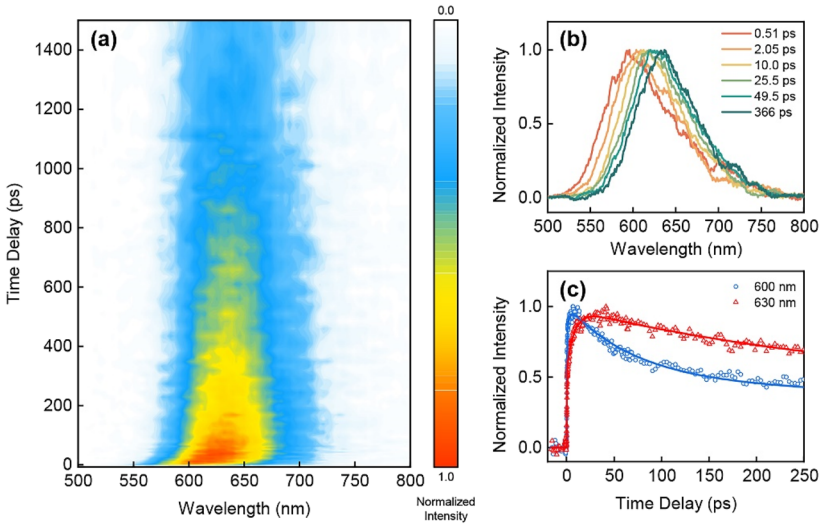

FIG. 4. (a) Waiting-time-dependent transient fluorescence spectra of 10^{-4} mol/l DCM ethanol solution under excitation of 400 nm. (b) Transient fluorescence spectra at various time delays represent the spectral redshift process after the photoexcitation. (c) Transient fluorescence dynamics probed at 600 nm (blue) and 630 nm (red). The dots denote the data points, while the curves denote the multiexponential fitting, accounting for the instrument response function (~100 fs).

DCM dye molecules dissolved in ethanol at a concentration of 10^{-4} mol/l. Figure 4(a) displays the detailed temporal evolution of the DCM fluorescence spectra, which have been corrected for chirp effects. Notably, the fluorescence intensity peak swiftly shifts toward longer wavelengths, transitioning from around 600 to ~630 nm within the initial 30 ps [Fig. 4(b)]. Examining the fluorescence dynamics at 630 nm reveals an initial rapid rise, characterized by a time constant of 4.4 ± 0.2 ps [Fig. 4(c)], attributed to the spectral redshift process. Following this rise to the maximum, the fluorescence dynamics demonstrate a bi-exponential decay process, featuring time constants τ_1 = 490 ± 60 ps and τ_2 > 2 ns. This ultrafast redshift of the DCM emission spectrum was previously observed using femtosecond up-conversion fluorescence spectroscopy[42] and femtosecond FNOPAS,[26] where it was interpreted as the consequence of the fast singlet excited state's energy reduction due to reorganization of the polar solvent molecules around the increased dipole moment following photoexcitation.

Previously, transient fluorescence spectra for an ethanol solution of rhodamine 6G at an optically diluted concentration as low as 10^{-5} mol/l were successfully recorded using an upgraded FNOPAS.[37] To further validate the improvement in signal-to-noise ratio while measuring weak transient fluorescence signals with the FCOPAS method, we conducted additional measurements on transient fluorescence spectra for ethanol solutions of DCM at optically diluted concentrations of 5 × 10^{-6} and 10^{-6} mol/l, respectively. Figure 5 depicts a comparison between the transient fluorescence spectra of DCM ethanol solutions acquired using two different collection schemes [the arc-shaped segment and the entire ring,

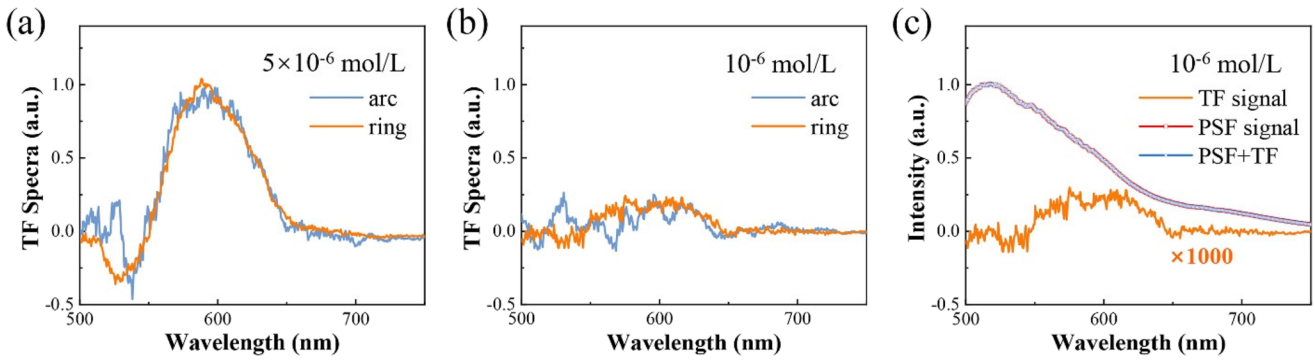

FIG. 5. Transient fluorescence (TF) spectra of (a) 5 × 10^{-6} mol/l and (b) 10^{-6} mol/l DCM ethanol solution collected from the arc-shaped segment (blue line) and the entire ring (orange line) of PSF. The excitation wavelength is 400 nm, and the time delay is fixed at 10 ps. (c) Comparison of the transient fluorescence signal, PSF background, and the combined signal prior to background subtraction (PSF + TF) collected from the entire ring during the analysis of the 10^{-6} mol/l DCM solution. This illustrates that the intensity of the PSF noise background exceeds that of the amplified fluorescence signal by three orders of magnitude.

similar to those utilized in Figs. 3(a) and 3(b)]. In this comparison, the time delay is fixed at 10 ps, and all data are averaged over 1000 repeated measurements (800 pulses per measurement).

In Fig. 5(a), the transient fluorescence of the DCM ethanol solution at a concentration of 5×10^{-6} mol/l displays a spectral shape similar to that obtained from the 10^{-4} mol/l solution at initial time delays. This outcome vividly illustrates a remarkable enhancement in the signal-to-noise ratio of the transient spectrum when amplifying across the entire PSF ring compared to a limited arc-shaped portion. Particularly noteworthy is the scenario when the solution is further diluted to a much lower concentration of 10^{-6} mol/l [Fig. 5(b)], wherein the transient fluorescence signal collected from the arc-shaped segment of the PSF becomes nearly indiscernible within the PSF noise. Conversely, capturing data from the entire ring maintains a distinctive transient fluorescence spectral feature. Figure 5(c) presents a comparison of the transient fluorescence signal, PSF background, and the combined signal before background subtraction collected from the entire ring during the analysis of the 10^{-6} mol/l DCM solution. This comparison illustrates that the intensity of the PSF noise background surpasses that of the amplified transient fluorescence (TF) signal by three orders of magnitude. Despite this significant background noise, the transient fluorescence spectrum can still be accurately resolved following background subtraction using the FCOPAS technique.

These findings reinforce the significant noise reduction capability of the FCOPAS method in contrast to traditional FNOPAS, where amplification is typically confined to a point-like area on the PSF ring. The FCOPAS presents a substantial advantage, delivering notably improved signal-to-noise ratios in practical fluorescence signal amplification measurements. Moreover, this method substantially improves fluorescence collection and amplification efficiency, resulting in a notably larger signal. These advantages collectively position FCOPAS as a more suitable approach for amplifying transient fluorescence, especially when dealing with significantly weaker fluorescence against a strong PSF background.

IV. CONCLUSION

Utilizing the phase-matching condition inherent in non-collinear OPA processes, we developed FCOPAS, a novel femtosecond time-resolved transient fluorescence technique. Unlike the traditional FNOPAS method, which employs lateral fluorescence collection and dot-like parametric amplification, FCOPAS introduces an innovative conical fluorescence collection and ring-like amplification scheme. Due to the stochastic intensity fluctuation properties of the PSF ring, FCOPAS achieves a substantial reduction of the PSF background to less than 1/1000 with 5-s averaging, representing an approximate order of magnitude improvement compared to previous FNOPAS results. This enhancement significantly improves signal-to-noise ratios in transient fluorescence amplification measurements. Notably, FCOPAS successfully resolves the transient fluorescence spectra of DCM dye molecules in ethanol at an optically dilute concentration of 10^{-6} mol/l, previously obscured within the PSF noise, now discernible with a favorable signal-to-noise ratio. These advancements position FCOPAS as a potent tool in ultrafast time-resolved fluorescence spectroscopic studies. It expands the scope for measuring exceedingly weak fluorescence dynamics across diverse samples, thereby enabling researchers to gain clearer insights into ultrafast phenomena within various photochemical and photophysical processes.

ACKNOWLEDGMENTS

This work was financially supported by the National Key Research and Development Program of China (Grant No. 2021YFA1201500), the National Natural Science Foundation of China (Grant Nos. 22027802 and 22222308), the CAS Project for Young Scientists and Basic Research (Grant No. YSBR-007), the Natural Science Foundation of Shandong Province (Grant No. ZR2021LLZ003), and the Strategic Priority Research Program of Chinese Academy of Sciences (Grant No. XDB33000000).

AUTHOR DECLARATIONS

Conflict of Interest

The authors declare that there are no conflicts of interest related to this article.

Author Contributions

E.C. and H.L. authors contributed equally to this work.

Ennan Cui: Data curation (equal); Formal analysis (lead); Investigation (equal); Writing – original draft (equal). **Heyuan Liu**: Data curation (equal); Investigation (equal); Visualization (lead). **Zhuan Wang**: Investigation (supporting); Methodology (supporting). **Hailong Chen**: Conceptualization (lead); Formal analysis (lead); Methodology (lead); Supervision (lead); Writing – original draft (equal). **Yu-Xiang Weng**: Conceptualization (supporting); Methodology (supporting); Supervision (supporting).

DATA AVAILABILITY

The data that support the findings of this study are available within the article.

REFERENCES

[1] J. R. Lakowicz, *Principles of Fluorescence Spectroscopy* (Springer, New York, 2006).
[2] R. van Grondelle, J. P. Dekker, T. Gillbro, and V. Sundstrom, Biochim. Biophys. Acta, Bioenerg. **1187**, 1 (1994).
[3] M. L. Horng, J. A. Gardecki, A. Papazyan, and M. Maroncelli, J. Phys. Chem. **99**, 17311 (1995).
[4] J. S. Baskin, H.-Z. Yu, and A. H. Zewail, J. Phys. Chem. A **106**, 9837 (2002).
[5] H.-Z. Yu, J. S. Baskin, and A. H. Zewail, J. Phys. Chem. A **106**, 9845 (2002).
[6] S.-H. Lim, T. G. Bjorklund, F. C. Spano, and C. J. Bardeen, Phys. Rev. Lett. **92**, 107402 (2004).
[7] F. Wang, G. Dukovic, L. E. Brus, and T. F. Heinz, Phys. Rev. Lett. **92**, 177401 (2004).
[8] T. Gustavsson, A. Bányász, E. Lazzarotto, D. Markovitsi, G. Scalmani, M. J. Frisch, V. Barone, and R. Improta, J. Am. Chem. Soc. **128**, 607 (2006).
[9] L. Ryderfors, E. Mukhtar, and L. B. A. Johansson, J. Phys. Chem. A **112**, 5794 (2008).
[10] Y. Pu, W. Wang, R. B. Dorshow, B. B. Das, and R. R. Alfano, Appl. Opt. **52**, 917 (2013).

[11] J. Xu, B. Chen, P. Callis, P. L. Muino, H. Rozeboom, J. Broos, D. Toptygin, L. Brand, and J. R. Knutson, J. Phys. Chem. B **119**, 4230 (2015).
[12] A. Sciortino, M. Gazzetto, M. L. Soriano, M. Cannas, S. Cardenas, A. Cannizzo, and F. Messina, Phys. Chem. Chem. Phys. **21**, 16459 (2019).
[13] Y. Liu, Z. Chen, X. Wang, S. Cao, J. Xu, R. Jimenez, and J. Chen, Phys. Chem. Chem. Phys. **22**, 19903 (2020).
[14] M. Gerecke, G. Bierhance, M. Gutmann *et al.*, Rev. Sci. Instrum. **87**, 053115 (2016).
[15] H. Chosrowjan, in *Encyclopedia of Spectroscopy and Spectrometry*, 3rd ed., edited by J. C. Lindon, G. E. Tranter, and D. W. Koppenaal (Academic Press, Oxford, 2017), p. 654.
[16] H. Mahr and M. D. Hirsch, Opt. Commun. **13**, 96 (1975).
[17] L. Zhao, J. Luis Pérez Lustres, V. Farztdinov, and N. P. Ernsting, Phys. Chem. Chem. Phys. **7**, 1716 (2005).
[18] I. Eom and T. Joo, J. Chem. Phys. **131**, 244507 (2009).
[19] T. Fujiwara, N. C. Romano, and E. C. Lim, Opt. Commun. **315**, 324 (2014).
[20] S. Arzhantsev and M. Maroncelli, Appl. Spectrosc. **59**, 206 (2005).
[21] C. Ma, W. M. Kwok, W. S. Chan, P. Zuo, J. T. Wai Kan, P. H. Toy, and D. L. Phillips, J. Am. Chem. Soc. **127**, 1463 (2005).
[22] B. Schmidt, S. Laimgruber, W. Zinth, and P. Gilch, Appl. Phys. B **76**, 809 (2003).
[23] K. Chen, J. K. Gallaher, A. J. Barker, and J. M. Hodgkiss, J. Phys. Chem. Lett. **5**, 1732 (2014).
[24] P. Fita, Y. Stepanenko, and C. Radzewicz, Appl. Phys. Lett. **86**, 021909 (2005).
[25] X.-H. Chen, X.-F. Han, Y.-X. Weng, and J.-Y. Zhang, Appl. Phys. Lett. **89**, 061127 (2006).
[26] Q. Ding, K. Meng, H. Yang, S. Wang, and Q. Gong, Opt. Commun. **284**, 3110 (2011).
[27] Q. Liao, Z. Xu, X. Zhong, W. Dang, Q. Shi, C. Zhang, Y. Weng, Z. Li, and H. Fu, J. Mater. Chem. C **2**, 2773 (2014).
[28] M. G. O. Gräfe, A. Hoffmann, and C. Spielmann, Appl. Phys. B **117**, 833 (2014).
[29] W. Dang, P. Mao, and Y. Weng, Rev. Sci. Instrum. **84**, 073105 (2013).
[30] J. Sung, P. Kim, B. Fimmel, F. Würthner, and D. Kim, Nat. Commun. **6**, 8646 (2015).
[31] R. Tempelaar, F. C. Spano, J. Knoester, and T. L. C. Jansen, J. Phys. Chem. Lett. **5**, 1505 (2014).
[32] X.-F. Han, X.-H. Chen, Y.-X. Weng, and J.-Y. Zhang, J. Opt. Soc. Am. B **24**, 1633 (2007).
[33] Y. Weng, X. Han, and J. Zhang, J. Opt. Soc. Am. B **25**, 1627 (2008).
[34] X.-F. Han, Y.-X. Weng, A. Pan, B. Zou, and J.-Y. Zhang, Appl. Phys. Lett. **92**, 032102 (2008).
[35] H.-L. Chen, Y.-X. Weng, and X.-Y. Li, Chin. J. Chem. Phys. **24**, 253 (2011).
[36] H. Chen, W. Dang, J. Xie, J. Zhao, and Y. Weng, Photosynth. Res. **111**, 81 (2012).
[37] P. Mao, Z. Wang, W. Dang, and Y. Weng, Rev. Sci. Instrum. **86**, 123113 (2015).
[38] J. P. Gordon, W. H. Louisell, and L. R. Walker, Phys. Rev. **129**, 481 (1963).
[39] D. A. Kleinman, Phys. Rev. **174**, 1027 (1968).
[40] S. Karan, S. Aarav, H. Bharadhwaj, L. Taneja, A. De, G. Kulkarni, N. Meher, and A. K. Jha, J. Opt. **22**, 083501 (2020).
[41] J. Lee Rodgers and W. A. Nicewander, Am. Stat. **42**, 59 (1988).
[42] S. Pommeret, T. Gustavsson, R. Naskrecki, G. Baldacchino, and J.-C. Mialocq, J. Mol. Liq. **64**, 101 (1995).